Optimisation of LRRK2 inhibitors and assessment of functional efficacy in cell-based models of neuroinflammation

ARTICLE *in* EUROPEAN JOURNAL OF MEDICINAL CHEMISTRY · MAY 2015

Impact Factor: 3.45 · DOI: 10.1016/j.ejmech.2015.03.003

9 AUTHORS, INCLUDING:

Lenka Munoz
University of Sydney
20 PUBLICATIONS **360** CITATIONS
SEE PROFILE

Benjamin Heng
Macquarie University
23 PUBLICATIONS **198** CITATIONS
SEE PROFILE

Gilles Guillemin
Macquarie University
248 PUBLICATIONS **5,227** CITATIONS
SEE PROFILE

Michael Kassiou
University of Sydney
232 PUBLICATIONS **3,089** CITATIONS
SEE PROFILE

European Journal of Medicinal Chemistry 95 (2015) 29–34

Contents lists available at ScienceDirect

European Journal of Medicinal Chemistry

journal homepage: http://www.elsevier.com/locate/ejmech

Short communication

Optimisation of LRRK2 inhibitors and assessment of functional efficacy in cell-based models of neuroinflammation

Lenka Munoz [a, 1], Madeline E. Kavanagh [b, 1], Athena F. Phoa [a], Benjamin Heng [c], Nicolas Dzamko [d, e], Ew-Jun Chen [a], Munikumar Reddy Doddareddy [f], Gilles J. Guillemin [c], Michael Kassiou [b, f, *]

[a] School of Medical Sciences, University of Sydney, NSW 2006, Australia
[b] School of Chemistry, University of Sydney, NSW 2006, Australia
[c] Australian School of Advanced Medicine, Macquarie University, NSW 2109, Australia
[d] School of Medical Sciences, University of New South Wales, Sydney, NSW 2052, Australia
[e] Neuroscience Research Australia, Randwick, NSW 2031, Australia
[f] Faculty of Health Sciences, University of Sydney, NSW 2006, Australia

ARTICLE INFO

Article history:
Received 16 September 2014
Received in revised form
1 March 2015
Accepted 2 March 2015
Available online 3 March 2015

Keywords:
LRRK2 inhibitors
Structure–activity relationships
Neuroinflammation

ABSTRACT

LRRK2IN1 is a highly potent inhibitor of leucine-rich repeat kinase 2 (LRRK2, IC_{50} = 7.9 nM), an established target for treatment of Parkinson's disease. Two LRRK2IN1 analogues **1** and **2** were synthesised which retained LRRK2 inhibitory activity (**1**: IC_{50} = 72 nM; **2**: IC_{50} = 51 nM), were predicted to have improved bioavailability and were efficacious in cell-based models of neuroinflammation. Analogue **1** inhibited IL-6 secretion from LPS-stimulated primary human microglia with EC_{50} = 4.26 μM. In order to further optimize the molecular properties of LRRK2IN1, a library of truncated analogues was designed based on docking studies. Despite lacking LRRK2 inhibitory activity, these compounds show anti-neuroinflammatory efficacy at micromolar concentration. The compounds developed were valuable tools in establishing a cell-based assay for assessing anti-neuroinflammatory efficacy of LRRK2 inhibitors. Herein, we present data that IL-1β stimulated U87 glioma cell line is a reliable model for neuroinflammation, as data obtained in this model were consistent with results obtained using primary human microglia and astrocytes.

1. Introduction

Leucine-rich repeat kinase (LRRK2) is a large (250 kDa) multi-domain serine–threonine kinase. Since the discovery that the gain-of-function LRRK2-G2019S mutant is linked to autosomal Parkinson's disease (PD), it has been one of the most investigated targets for treating PD [1]. In the central nervous system (CNS), LRRK2 induces neuronal apoptosis by up regulating the mRNA expression and formation of pro-apoptotic factors, such as Bim, FasL and caspases 3, 8, and 9 [2]. LRRK2 contributes to the formation of Lewy body pathology through phosphorylation-dependent aggregation of proteins and by inhibiting the ubiquitin-proteosomal route of protein clearance [3,4]. Furthermore, LRRK2 disrupts neuronal morphology, vesicular homeostasis, as well as the synaptic concentration, release and recycling of dopamine [5]. Recent studies have demonstrated that LRRK2 inhibition attenuates microglial inflammatory responses *via* inhibiting signalling pathways down-stream of toll-like receptors (TLR) [6–8]. The engagement of LRRK2 in the inflammatory pathways [9] indicates that LRRK2 might not only be involved in PD, but also in a number of CNS disorders where neuroinflammation is a part of disease pathophysiology, such as Alzheimer's disease, multiple sclerosis, neuropathic pain and depression [10–12].

Several potent, non-selective tool compounds, including staurosporine (LRRK2: IC_{50} = 1–2 nM) [13], sunitinib (LRRK2: IC_{50} = 79 nM) [14] and ROCK inhibitor H-1152 (LRRK2: IC_{50} = 244 nM) [14] provided preliminary support for LRRK2 inhibition as a potential therapeutic option for PD. Subsequent studies focused on developing inhibitors selective for LRRK2.

* Corresponding author. School of Chemistry, University of Sydney, NSW 2006, Australia.
E-mail address: michael.kassiou@sydney.edu.au (M. Kassiou).
[1] Contributed equally to the work.

http://dx.doi.org/10.1016/j.ejmech.2015.03.003
0223-5234/

Numerous compounds displayed LRRK2 inhibitory potency (K_i/IC_{50} < 100 nM), however the majority lacked the ability to cross the blood–brain barrier (BBB) [15]. The first compound capable of inhibiting LRRK2 activity in the CNS was amino-pyrimidine derivative GNE-7915, which was both potent (K_i = 1 nM, IC_{50} = 9 nM) and LRRK2-selective (1/187 and 10/392 kinases inhibited with IC_{50} < 100 nM) [16]. Given the important role for LRRK2 in PD and neuroinflammation, the search for potent and BBB-permeable LRRK2 inhibitors continues and is the subject of the work presented here.

2. Results and discussion

We have chosen LRRK2 inhibitor, LRRK2IN1 as a lead to develop bioavailable and BBB-permeable LRRK2 inhibitors. LRRK2IN1 is potent against both the wild-type LRRK2 (IC_{50} = 13 nM) and mutant LRRK2-G2019S (IC_{50} = 6 nM) [17]. It is selective for LRRK2, interacting with only 12 of 470 other kinases, and with only 5 kinases at sub-micromolar concentrations. LRRK2IN1 is neuroprotective *in vitro* and inhibits the activity of LRRK2 in kidney and spleen when administered *in vivo*. However, LRRK2IN1 is not able to cross the BBB, which halted further clinical development of this compound. We used *in silico* approach (Schrödinger, LLC) to assess the physicochemical and pharmacokinetic properties of LRRK2IN1 that might be responsible for poor CNS permeability. Oxidative metabolism by cytochrome p450 enzymes, dealkylation and/or aromatic hydroxylation reactions were predicted to occur at six sites on LRRK2IN1 (Fig. 1). Analysis of the LRRK2IN1 metabolite resulting from these reactions indicated that metabolite(s) would be unlikely to cross the BBB. This was demonstrated through the reduced lipophilicity (cLogP), increased topological polar surface area (tPSA), poor predicted oral absorption (F) and low MDCK cell permeability (model of BBB penetration, Fig. 1).

We proposed that limiting the metabolism of LRRK2IN1 by incorporating bioisosteric substituents, as suggested in structures **1** and **2** (Fig. 1) would improve physicochemical properties of LRRK2IN1 and increase potential CNS penetration. A homology model of the LRRK2 kinase domain was constructed using Lymphocyte specific kinase (Lck) as a structural template (PDB 1qpc, Fig. 2). The crystal structure of Lck was selected because of the high homology between the amino acid sequences of the Lck and LRRK2 active sites, the high resolution (1.6 Å) of the structure and the presence of a relevant co-crystallised substrate (phosphoaminophosphonic acid-adenylate ester) [18]. The integrity of the homology model and its binding predictions were validated by *in silico* screening of libraries of kinase inhibitors.

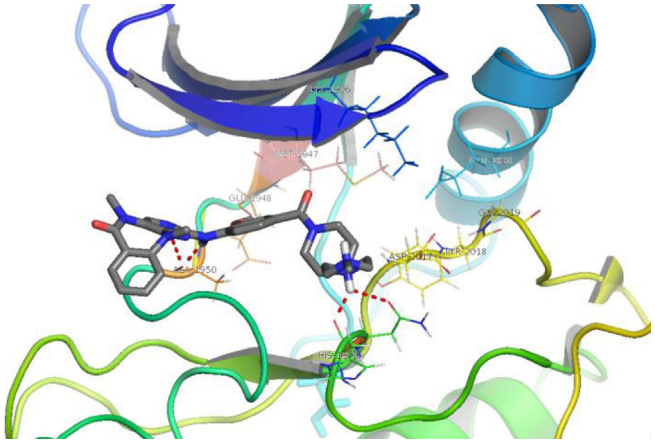

Fig. 2. LRRK2IN1 docked into LRRK2 homology model. LRRK2IN1 binds to the kinase active site cleft by forming hydrogen-binding interactions (red dashes) between the pyrimidinyl-aniline motif and the adenine binding hinge residue Ala1950. The protonated piperazine of LRRK2IN1 was predicted to form interactions with His1998 and Asn1999 residues. Other key active site residues are also shown, including the Met1947 gatekeeper residue (orange), DF(Y)G activation loop (yellow), and catalytic residues Lys1906 and Glu1920 (blue). Homology model constructed and docking performed using Schrödinger suite software (Prime, v3.1, Impact, v5.8, LigPrep v2.5, Glide v5.6, Schrödinger, LLC). (For interpretation of the references to colour in this figure legend, the reader is referred to the web version of this article.)

LRRK2IN1 and a series of designed analogues were docked into the homology model. Key interactions identified were hydrogen bonding between the pyrimidine ring-N atoms and aniline of LRRK2IN1 and the kinase hinge residues Glu1948 and Ala1950 (Fig. 2). Hydrogen bonding between the protonated piperazinium group and His1998 or Asn1999, which lie in close proximity to the

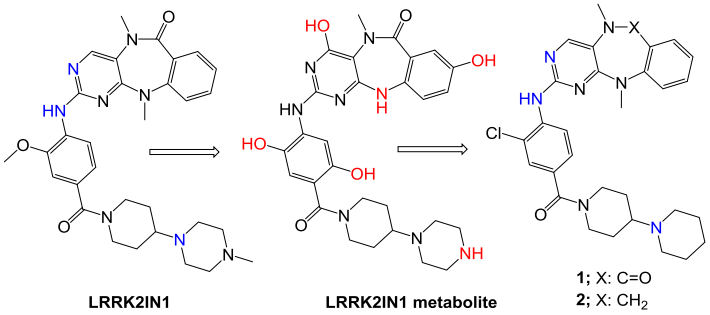

	M_w	cLogP	tPSA (Å^2)	F (%)	MDCK (nm/s)	Predicted metabolites
LRRK2IN1	570.7	2.8	106	50 (49.3)[a]	27	6
LRRK2IN1 metabolite	576.6	-0.4	215	0	0.05	-
1	560.1	4.4	93	84	293	2
2	546.1	5.6	69	83	653	4

[a] Experimentally determined bioavailability.[17]

Fig. 1. Predicted molecular properties of LRRK2IN1, predicted metabolite and analogues 1–2. Primary sites of oxidative metabolism (red) and tabulated molecular properties were predicted using QikProp v3.5 (Schrödinger, LLC, 2012). Functional groups important for binding interactions (blue) were predicted using Glide v5.6 (Schrödinger, LLC, 2010). (For interpretation of the references to colour in this figure legend, the reader is referred to the web version of this article.)

DF(Y)G activation loop, were also identified. Docking of analogues **1** and **2** predicted that key binding interactions were conserved which provided confidence that structural alterations made to the LRRK2IN1 scaffold in these analogues would not affect inhibitor binding. *In silico* assessment of physicochemical properties indicated that bioisosteric substituents should improve the metabolic stability and BBB permeability of analogues **1**–**2** (Fig. 1).

Analogues **1** and **2** were synthesised by a convergent route. Diazepinone **10** and diazepine **14** were synthesised from functionalised pyrimidine **5**, which itself was obtained by the nitration and chlorination of uracil **3** (Scheme 1). Ullman-type nucleophilic aromatic substitution of aniline **6** with aqueous methylamine, followed by Fischer esterification, gave ester precursor **8**. Substitution reaction of dichloropyrimidine **5** with **8** afforded the nitrobenzoate intermediate **9**. Tandem nitro-reduction-aminolysis of **9** afforded diazepinone **10**, which was subsequently methylated to give **11**. Diazepine **15** was synthesised by a similar route, substituting 2-aminobenzaldehyde **12** in place of ester **8**. Tandem nitro reduction–reductive amination using Adam's catalyst was found to be an efficient route to diazepine **14**, which was subsequently methylated to give **15** [19]. The 1,4′-bipiperidin-1′-yl-aniline **21** was obtained from the reductive amination of *tert*-butyl carbamate (boc)-protected piperidone **16** and piperidine **17**. Boc-deprotection and amide coupling with benzoic acid **20** afforded aniline fragment **21**. Buchwald–Hartwig amination was used as the final reaction to yield LRRK2IN1 analogues **1** and **2** (Scheme 2), which were assessed for *in vitro* inhibition of mutant LRRK2-G2019S [17]. In accordance with docking predictions, analogues **1**–**2** inhibited LRRK2-G2019S with IC_{50} of 72 and 51 nM, respectively (Table 1). In our hands LRRK2IN1 was found to inhibit LRRK2-G2019S with IC_{50} of 7.9 nM, suggesting that changes leading to more stable analogues caused only marginal loss in inhibiting LRRK2.

Despite the large number of new LRRK2 inhibitors reported in the literature, evaluation of these inhibitors involves

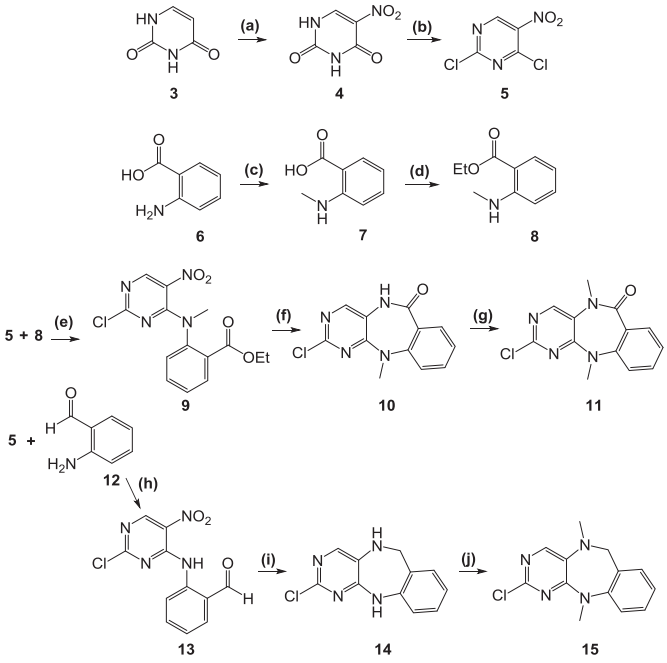

Scheme 1. Synthesis of diazepinone and diazepine coupling partners. Reagents and conditions: (a) H_2SO_4, HNO_3, 50 °C, 3 h, 92%; (b) $POCl_3$, *N,N*-dimethylaniline, reflux, 3 h, 43%; (c) $MeNH_2$, Cu(0), 100 °C, 20 h, sealed tube, 89%; (d) EtOH, H_2SO_4, reflux, 18 h, quant.; (e) DIPEA, 1,4-dioxane, 55 °C, 3 h, 57%; (f) Fe powder, AcOH, 50 °C, 9 h, 58%; (g) NaH, MeI, DMA, −10 to 0 °C, 1.5 h, quant.; (h) DIPEA, 1,4-dioxane, 65 °C, 1.75 h, 78%; (i) PtO_2, H_2 (1 atm), MeOH, reflux, 48 h, 99% (j) NaH, MeI, DMA, −10 to 0 °C, 1.5 h, quant.

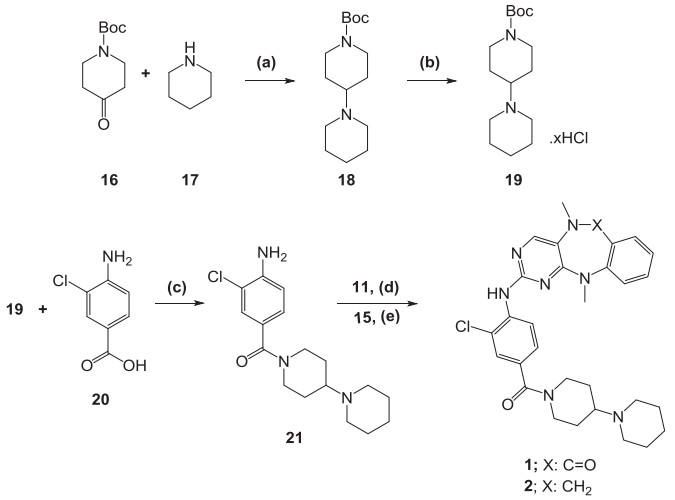

Scheme 2. Synthesis of aniline 21 and coupling of analogues 1–2. Reagents and conditions: (a) AcOH, $Na(OAc)_3BH$, DCE, 0 °C to RT, overnight, 25%; (b) 4 M HCl in 1,4-dioxane, RT, 1 h, quant.; (c) EDCI, HOBt, DIPEA, DCM, RT, 20 h, 93%; (d) $Pd_2(dba)_3$, X-Phos, ^tBuOK, 1,4-dioxane, 60 °C, 21 h, 39%; (e) $Pd_2(dba)_3$, X-Phos, Cs_2CO_3, 1,4-dioxane, reflux, 6 h, 3%.

Table 1
Biochemical and cell-based activities of LRRK2 inhibitors.

	LRRK2-G2019S (IC_{50}, nM)[a]	IL-6 inhibition at 10 μM (%)[a]	
		Primary human microglia	U87 glioma cells
LRRK2IN1	7.9 ± 2.3	95.0 ± 1.2 (*EC_{50} = 0.83 ± 0.4 μM*)	94.14 ± 0.7 (*EC_{50} = 0.66 ± 0.1 μM*)
1	72.0 ± 2.5	81.3 ± 7.8 (*EC_{50} = 4.26 ± 0.1 μM*)	87.9 ± 5.1 (*EC_{50} = 3.68 ± 0.6 μM*)
2	51.2 ± 16.4	70.0 ± 8.9	58.8 ± 8.3
11	>1000	18.0 ± 4.9	23.2 ± 2.2
15	>1000	6.3 ± 1.1	64.6 ± 4.4
21	654 ± 286	16.9 ± 7.5	49.9 ± 9.1

The values in italics indicates those compounds which should an inhibition greater than 80% a full dose response was determined which is represented by the EC50.
[a] Assays were performed as described in Ref. [17] (LRRK2-G2019S *in vitro* assay), ref [20] (microglia) and ref [21] (U87). Data are mean ± SEM from 2–4 independent experiments performed in duplicates. For details see Supplementary material.

predominantly *in vitro* kinase assays. Functional efficacy data are often missing, mostly due to the lack of high-throughput, LRRK2-dependent and disease-relevant assays. Because LRRK2 regulates neuroinflammatory signalling pathways [6–8], we used primary human microglia to assess cellular efficacy of LRRK2IN1 analogues. Lipopolysaccharide (LPS) stimulates microglia by binding to TLR4, which induces the production of inflammatory cytokines such as IL-1β, TNFα and IL-6 through activation of the p38 MAPK pathway [6]. Activation of TLR4 also induces MyD88-dependent activation of LRRK2 and *in vitro* [7], LRRK2 phosphorylates MKK3/6, which are upstream activators of p38 MAPK [22]. These data, together with the fact that knock-down of LRRK2 reduced the phosphorylation of p38 MAPK [8], suggest that microglial LRRK2 regulates p38 MAPK signalling down-stream of TLR4. IL-6 was chosen as an endpoint, because this cytokine is over-expressed in the brain of PD patients [23] and is regulated by p38 MAPK signalling [20]. The improved biochemical index (BE = *in vitro* IC_{50}/cellular EC_{50}) of analogue **1** (BE = 0.017) compared to LRRK2IN1 (BE = 0.009), suggested that structural changes made to improve bioavailability had been favourable and that further improvement in the molecular properties of LRRK2IN1 analogues result in an inhibitor with required the BE of 0.4 (as calculated for the majority of marketed drugs) [24]. Analogue **2** also inhibited IL-6 secretion (70% inhibition at 10 μM) in

accordance with the compound's activity against LRRK2-G2019S (IC_{50} = 51.2 ± 16.4 nM).

As LRRK2 activation downstream of TLR4 is MyD88-dependent [7], we also sought to investigate if LRRK2 inhibitors block MyD88-dependent signalling down-stream of IL-1 receptor. Post-mortem analysis of the substantia nigra from PD patients reported increased IL-1β levels [23], making IL-1β a PD-relevant stimuli of IL-6. We chose the U87 glioma cell line as it is of glial origin, expresses LRRK2 (data not shown) and secretes IL-6 in response to IL-1β stimulation [21]. LRRK2IN1 and analogue **1** inhibited IL-6 secretion in IL-1β stimulated U87 cells with EC_{50} = 0.66 and 3.68 μM, respectively. These values are nearly identical with potency in primary human microglia (Table 1). Finally, we tested LRRK2IN1 and **1** for their efficacy in primary human astrocytes (Fig. 3A). IL-6 secretion from IL-1β stimulated astrocytes was reduced by 73.9 ± 2.3% with LRRK2IN1 (10 μM) and by 67.2 ± 9.3% with analogue **1** (10 μM), suggesting that LRRK2 is also engaged in the inflammatory pathways in astrocytes, although to a lesser extent.

The aniline **21** and diazepinone/diazepine fragments **11** and **15** were also tested for their LRRK2 inhibitory potency (Table 1). While **11** and **15** were inactive at 1 μM, aniline **21** inhibited LRRK2-G2019S with IC_{50} = 654 nM. Because of the modest inhibitory activity, low molecular weight and predicted metabolic stability of **21**, we proposed to use this fragment as a lead to develop a truncated series of LRRK2IN1 analogues to further improve physicochemical properties. Docking studies of LRRK2IN1 and analogues **1** and **2** had previously indicated that only the pyrimidine ring of the diazepinone/diazepine moiety was important for hydrogen bonding interactions. Consequently, we proposed to replace the diazepinone/diazepine group with simple aliphatic, aromatic or heteroaromatic substituents. Molecular modelling was used to evaluate the physicochemical properties of prospective analogues. Docking studies, using the previously described LRRK2 homology model, suggested that proposed analogues would retain a similar binding pose to the lead structures LRRK2IN1, **1** and **2** in the LRRK2 active site.

Nineteen analogues **22**–**40** were synthesised by employing a series of key reactions to couple aniline **21** with appropriate electrophiles. Six-membered aromatic analogues **22**–**32** were synthesised under Buchwald–Hartwig reaction conditions (Scheme 3(i)). *N*-benzyl analogues **33**–**36** were prepared from aniline **21** and the respective benzyl bromide by heating to reflux in a minimal

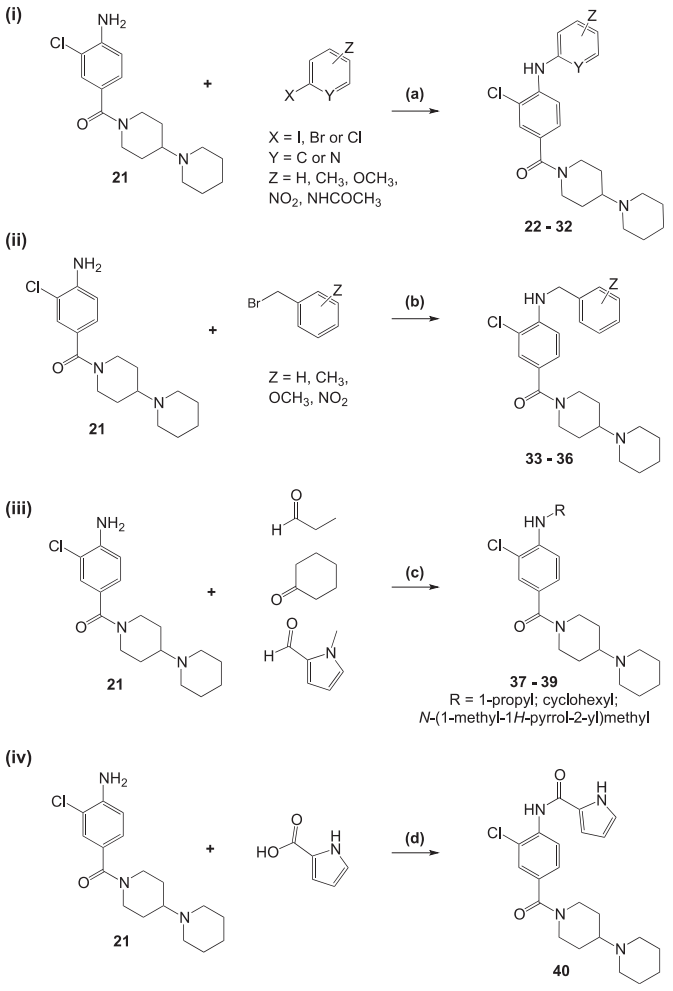

Scheme 3. Synthesis of truncated analogues 22–40. Reagents and conditions: (a) $Pd_2(dba)_3$, X-Phos, Cs_2CO_3, 1,4-dioxane, reflux, 2–6 h; (b) water, reflux, 2.5–5 h; (c) AcOH, $Na(OAc)_3BH$, DCE, 0 °C to RT, 20–48; (d) oxalyl chloride, 50 °C then Et_3N, DCM, 0 °C to RT, 24 h, then DMAP, RT, 20 h. Yields for each product are listed in Table 2.

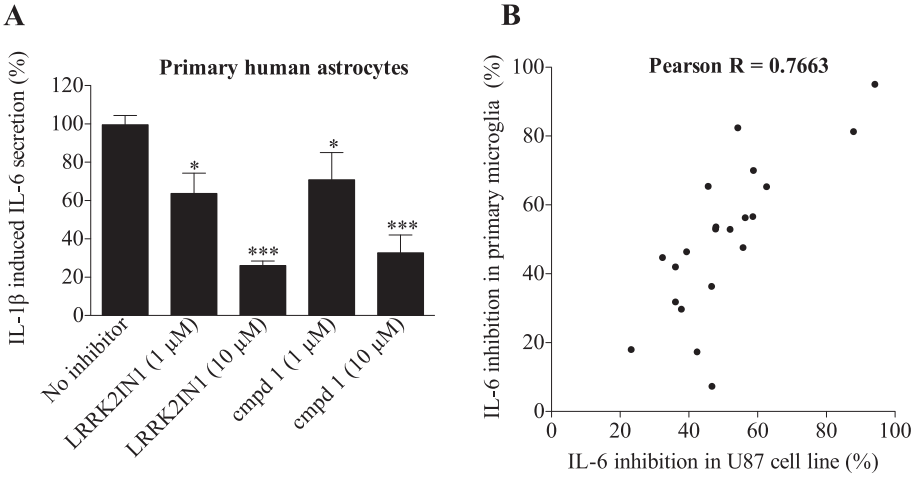

Fig. 3. (A) LRRK2 inhibitors attenuate IL-6 secretion from primary human astrocytes. Data are mean ± SEM from five independent experiments performed in duplicates (1-way ANOVA followed by Newman–Keuls test, *P < 0.05; ***P < 0.001). For details see Supplementary material. (B) Non-parametric Pearson correlation test (GraphPad Prism 5) of values presented in Tables 1–2 demonstrates correlation between efficacy in primary human microglia and U87 glioma cell line.

Table 2
Yields, biochemical and cell-based activities of truncated analogues 22–40.

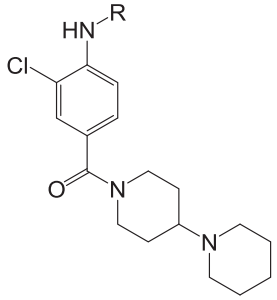

	R	Yield (%)	LRRK2-G2019S (IC_{50}, nM)[1]	IL-6 inhibition at 10 μM (%)[1]	
				Microglia	U87
22		27	>1000	46.4 ± 13.1	39.3 ± 7.2
23		12	>1000	ND	40.7 ± 6.2
24		66	>1000	7.3 ± 8.8	46.7 ± 3.3
25		47	>1000	36.3 ± 10.2	46.6 ± 10.7
26		71	>1000	44.7 ± 23.2	32.3 ± 5.7
27	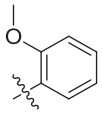	99	>1000	56.6 ± 11.5	58.6 ± 4.2
28	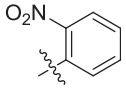	91	>1000	65.4 ± 15.6	45.6 ± 5.3
29	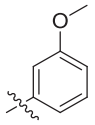	94	>1000	53.0 ± 9.2	47.8 ± 8.3
30	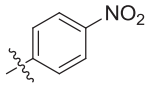	98	>1000	53.6 ± 7.1	47.9 ± 7.5
31	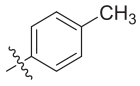	99	>1000	29.7 ± 10.7	37.8 ± 0.9
32	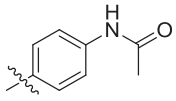	45	>1000	31.8 ± 9.3	36.1 ± 6.7
33	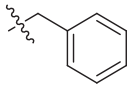	60	>1000	65.3 ± 7.8	62.6 ± 0.7
34	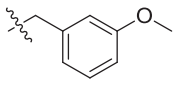	42	>1000	52.9 ± 13.0	52.0 ± 6.7

Table 2 (*continued*)

	R	Yield (%)	LRRK2-G2019S (IC_{50}, nM)[1]	IL-6 inhibition at 10 μM (%)[1]	
				Microglia	U87
35	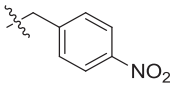	15	>1000	56.3 ± 11.2	56.4 ± 5.6
36	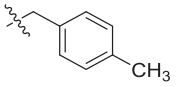	21	>1000	42.0 ± 19.5	36.1 ± 6.8
37	1-propyl	28	>1000	47.6 ± 11.6	55.8 ± 3.9
38		12	>1000	82.4 ± 4.0	54.2 ± 2.9
39	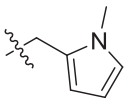	37	>1000	17.3 ± 12.3	42.4 ± 6.7
40	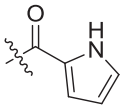	14	>1000	no inh.	51.9 ± 6.7

[1] Assays were performed as described in Ref. [17] (LRRK2-G2019S *in vitro* assay), ref [20] (microglia) and ref [21] (U87). Data are mean ± SEM from 2–4 independent experiments performed in duplicates. For details see Supplementary material.

quantity of water (Scheme 3(ii)) [25]. Aliphatic analogues *N*-propylamine **37** and cyclohexylamine **38** were synthesized by reductive amination from the respective aldehyde or ketone precursor (Scheme 3(iii)). Pyrrole analogues containing a methylamine (**39**) or amide (**40**) linker were afforded by reductive amination, or amide coupling *via* an acid chloride intermediate, respectively (Scheme 3(iii) and 3(iv)).

Truncated analogues **22**–**40** were assessed for biochemical inhibition of LRRK2-G2019S *in vitro* and cellular efficacy in primary human microglia and U87 cells (Table 2). No inhibition of LRRK2-G2019S was detected for any of the truncated analogues when screened at 1 μM. In comparison, truncated analogues continued to show modest anti-IL-6 efficacy, comparable to that of the unsubstituted aniline **21**. This data indicated that substitution of aniline **21** was detrimental to LRRK2 inhibition, but not to the anti-inflammatory efficacy. In particular, analogue **38** was found to inhibit LPS-induced IL-6 secretion from microglia by 83% when screened at 10 μM, which was equivalent to the efficacy of LRRK2 inhibitor **1** (Table 1). Because of the relevance of anti-inflammatory compounds in the treatment of CNS disorders, the off-target activity and anti-inflammatory efficacy of **38** is under further investigation. Despite lacking inhibitory activity against LRRK2-G2019S, the anti-inflammatory efficacy of truncated analogues **22**–**40** significantly correlated between primary human microglia and U87 cells (Table 2, Fig. 3B). This correlation, also observed for LRRK2IN1 and inhibitors **1**–**2** (Table 1, Fig. 3B), provided evidence that the IL-1β-stimulated U87 cell line is a reliable method for both assessing the efficacy of LRRK2 inhibitors and also, the efficacy of other anti-inflammatory compounds. This is particularly important in the early stages of the drug discovery where the screening of compound libraries in primary human cells is not feasible.

3. Conclusion

In summary, novel LRKK2 inhibitors **1**–**2** with anti-neuroinflammatory efficacy and promising molecular properties

have been developed. These compounds have been used to validate the use of primary human microglia and U87 cells to assess the functional efficacy of LRRK2 inhibitors. A series of truncated analogues with moderate anti-neuroinflammatory efficacy have also been synthesised and used to demonstrate consistency between microglia and U87 cellular assays. The molecular target of truncated analogues is under investigation. The compounds and assays developed in this study are valuable in light of the significant role of neuroinflammation in PD and a broad range of CNS disorders.

Acknowledgements

This study was supported by a grant from Parkinson's NSW Foundation (MK and LM) and the University of Sydney Brown Fellowship (LM). GJG is supported by the Australian Research Council (FT120100397), Cure Brain Cancer Foundation, Tour de Cure Foundation and St Vincent's Clinic Foundation. ND is a CJ Martin Fellow of the National Health and Medical Research Council of Australia.

Appendix A. Supplementary data

Supplementary data related to this article can be found at http://dx.doi.org/10.1016/j.ejmech.2015.03.003.

References

[1] M. Funayama, K. Hasegawa, H. Kowa, M. Saito, S. Tsuji, F. Obata, A new locus for Parkinson's disease (PARK8) maps to chromosome 12p11.2-q13.1, Ann. Neurol. 51 (2002) 296–301.
[2] C.Y. Chen, Y.H. Weng, K.Y. Chien, K.J. Lin, T.H. Yeh, Y.P. Cheng, C.S. Lu, H.L. Wang, (G2019S) LRRK2 activates MKK4-JNK pathway and causes degeneration of SN dopaminergic neurons in a transgenic mouse model of PD, Cell. Death Differ. 19 (2012) 1623–1633.
[3] M. Devine, H. Plun-Favreau, N. Wood, Parkinson's disease and cancer: two wars, one front, Nat. Rev. Cancer 11 (2011) 812–823.
[4] M. Lichtenberg, A. Mansilla, V.R. Zecchini, A. Fleming, D.C. Rubinsztein, The Parkinson's disease protein LRRK2 impairs proteasome substrate clearance without affecting proteasome catalytic activity, Cell. Death Dis. 2 (2011) e196.
[5] B.D. Lee, V.L. Dawson, T.M. Dawson, Leucine-rich repeat kinase 2 (LRRK2) as a potential therapeutic target in Parkinson's disease, Trends Pharmacol. Sci. 33 (2012) 365–373.
[6] M.S. Moehle, P.J. Webber, T. Tse, N. Sukar, D.G. Standaert, T.M. DeSilva, R.M. Cowell, A.B. West, LRRK2 inhibition attenuates microglial inflammatory responses, J. Neurosci. 32 (2012) 1602–1611.
[7] N. Dzamko, F. Inesta-Vaquera, J. Zhang, C. Xie, H. Cai, S. Arthur, L. Tan, H. Choi, N. Gray, P. Cohen, P. Pedrioli, K. Clark, D.R. Alessi, The IkappaB kinase family phosphorylates the Parkinson's disease kinase LRRK2 at Ser935 and Ser910 during Toll-like receptor signaling, PLoS One 7 (2012) e39132.
[8] B. Kim, M.-S. Yang, D. Choi, J.-H. Kim, H.-S. Kim, W. Seol, S. Choi, I. Jou, E.-Y. Kim, E.-H. Joe, Impaired inflammatory responses in murine LRRK2-knockdown brain microglia, PLoS One 7 (2012) e34693.
[9] N. Dzamko, G. Halliday, An emerging role for LRRK2 in the immune system, Biochem. Soc. Trans. 40 (2012) 1134–1139.
[10] L. Munoz, A.J. Ammit, Targeting p38 MAPK pathway for the treatment of Alzheimer's disease, Neuropharmacology 58 (2010) 561–568.
[11] A.K. Walker, A. Kavelaars, C.J. Heijnen, R. Dantzer, Neuroinflammation and comorbidity of pain and depression, Pharmacol. Rev. 66 (2014) 80–101.
[12] E. Ellwardt, F. Zipp, Molecular mechanisms linking neuroinflammation and neurodegeneration in MS, Exp. Neurol. (2014), http://dx.doi.org/10.1016/j.expneurol.2014.02.006.
[13] B. Lee, J.-H. Shin, J. VanKampen, L. Petrucelli, A. West, H. Ko, Y.-I. Lee, K. Maguire-Zeiss, W. Bowers, H. Federoff, V. Dawson, T. Dawson, Inhibitors of leucine-rich repeat kinase-2 protect against models of Parkinson's disease, Nat. Med. 16 (2010) 998–1000.
[14] J. Nichols, N. Dzamko, J. Hutti, L. Cantley, M. Deak, J. Moran, P. Bamborough, A.D. Reith, D.R. Alessi, Substrate specificity and inhibitors of LRRK2, a protein kinase mutated in Parkinson's disease, Biochem. J. 424 (2009) 47–60.
[15] M.E. Kavanagh, M.R. Doddareddy, M. Kassiou, The development of CNS-active LRRK2 inhibitors using property-directed optimisation, Bioorg Med. Chem. Lett. 23 (2013) 3690–3696.
[16] A.A. Estrada, X. Liu, C. Baker-Glenn, A. Beresford, D.J. Burdick, M. Chambers, B.K. Chan, H. Chen, X. Ding, A.G. DiPasquale, S.L. Dominguez, J. Dotson, J. Drummond, M. Flagella, S. Flynn, R. Fuji, A. Gill, J. Gunzner-Toste, S.F. Harris, T.P. Heffron, T. Kleinheinz, D.W. Lee, C.E. Le Pichon, J.P. Lyssikatos, A.D. Medhurst, J.G. Moffat, S. Mukund, K. Nash, K. Scearce-Levie, Z. Sheng, D.G. Shore, T. Tran, N. Trivedi, S. Wang, S. Zhang, X. Zhang, G. Zhao, H. Zhu, Z.K. Sweeney, Discovery of highly potent, selective, and brain-penetrable leucine-rich repeat kinase 2 (LRRK2) small molecule inhibitors, J. Med. Chem. 55 (2012) 9416–9433.
[17] X. Deng, N. Dzamko, A. Prescott, P. Davies, Q. Liu, Q. Yang, J. Lee, M. Patricelli, T. Nomanbhoy, D. Alessi, N. Gray, Characterization of a selective inhibitor of the Parkinson's disease kinase LRRK2, Nat. Chem. Biol. 7 (2011) 203–205.
[18] X. Zhu, J. Kim, J. Newcomb, P. Rose, D. Stover, L. Toledo, H. Zhao, K. Morgenstern, Structural analysis of lymphocyte-specific kinase Lck in complex with non-selective and Src family selective inhibitors, Structure 7 (1999) 651–661.
[19] T. Reekie, M.E. Kavanagh, M. Longworth, M. Kassiou, Synthesis of biologically active seven-membered-ring heterocycles, Synthesis 45 (2013) 3211–3227.
[20] Y. Yeung, N. Bryce, S. Adams, N. Braidy, M. Konayagi, K. McDonald, C. Teo, G. Guillemin, T. Grewal, L. Munoz, p38 MAPK inhibitors attenuate pro-inflammatory cytokine production and invasiveness of human U251 glioblastoma cells, J. Neurooncol. 109 (2012) 35–44.
[21] F. Gurgis, Y.T. Yeung, M. Tang, B. Heng, M. Buckland, A. Ammit, J. Haapasalo, H. Haapasalo, G. Guillemin, T. Grewal, L. Munoz, The p38-MK2-HuR pathway potentiates EGFRvIII-IL-1β driven IL-6 secretion in glioblastoma cells, Oncogene (2014), http://dx.doi.org/10.1038/onc.2014.225.
[22] C.J. Gloeckner, A. Schumacher, K. Boldt, M. Ueffing, The Parkinson disease-associated protein kinase LRRK2 exhibits MAPKKK activity and phosphorylates MKK3/6 and MKK4/7, in vitro, J. Neurochem. 109 (2009) 959–968.
[23] L.M. Collins, A. Toulouse, T.J. Connor, Y.M. Nolan, Contributions of central and systemic inflammation to the pathophysiology of Parkinson's disease, Neuropharmacology 62 (2012) 2154–2168.
[24] D.C. Swinney, J. Anthony, How were medicines discovered? Nat. Rev. Drug Disc. 10 (2011) 507–519.
[25] D. Kommi, D. Kumar, R. Bansal, R. Chebolu, A. Chakraborti, "All-water" chemistry of tandem N-alkylation-reduction-condensation for synthesis of N-arylmethyl-2-substituted benzimidazoles, Green Chem. 14 (2012) 3329–3335.